The different energy loss mechanisms of inclusive and b-tagged reconstructed jets within ultra-relativistic heavy-ion collisions

F. Senzel[a,*], J. Uphoff[a], Z. Xu[b], C. Greiner[a,**]

[a] *Institut für Theoretische Physik, Goethe-Universität Frankfurt, Max-von-Laue-Str. 1, D-60438 Frankfurt am Main, Germany*
[b] *Department of Physics, Tsinghua University and Collaborative Innovation Center of Quantum Matter, Beijing 100084, China*

arXiv:1602.05086v2 [hep-ph] 18 Nov 2016

Abstract

The phenomenon of jet quenching provides essential information about the properties of hot and dense matter created in ultra-relativistic heavy-ion collisions. Recent results from experiments at the Large Hadron Collider (LHC) show evidence for an unexpectedly similar suppression of both light and heavy flavor jets. Furthermore, the role of radiative energy loss of heavy quarks is still under active discussion within the theoretical community. By employing the parton cascade *Boltzmann Approach to Multi-Parton Scatterings* (BAMPS), which numerically solves the 3+1D Boltzmann equation both for light and heavy flavor partons, we calculate the nuclear modification factor of inclusive and b-tagged reconstructed jets in 0-10% central $\sqrt{s}_{\mathrm{LHC}} = 2.76\,\mathrm{A\,TeV}$ Pb + Pb collisions. Based on perturbative QCD cross sections we find a rather similar suppression of light and heavy flavor jets. To further investigate light and heavy flavor energy loss we predict the R dependence of inclusive and b-tagged jet suppression. Furthermore, we propose the medium modification of b-tagged jet shapes as an observable for discriminating between different heavy quark energy loss scenarios.

As proposed by Bjorken in the early 1980s [1] quenched jets—particles with high transverse momentum p_t—represent an excellent probe for investigating the hot and dense matter created in ultra-relativistic heavy-ion collisions called the quark-gluon plasma (QGP) [2, 3]. Created under well theoretical control by perturbative quantum-chromodynamics (pQCD) in hard nucleon-nucleon collisions, jets lose energy and momentum while traversing the QGP. Due to their early creation they witness a large part of the QGP evolution and thereby provide essential information about the underlying medium.

Before the era of the Large Hadron Collider (LHC) at CERN, the most prominent observable for studying jet quenching was the suppression of inclusive hadron spectra quantified by the nuclear modification factor R_{AA},

$$R_{AA} = \frac{\mathrm{d}^2 N_{\mathrm{AA}}/\mathrm{d}p_T\mathrm{d}y}{N_{\mathrm{bin}}\,\mathrm{d}^2 N_{\mathrm{pp}}/\mathrm{d}p_T\mathrm{d}y}\,. \tag{1}$$

Results from both $\sqrt{s}_{\mathrm{RHIC}} = 200\,\mathrm{A\,GeV}$ Au + Au collisions at the Relativistic Heavy-Ion Collider (RHIC) [4, 5] and $\sqrt{s}_{\mathrm{LHC}} = 2.76\,\mathrm{A\,TeV}$ Pb + Pb collisions at the LHC [6, 7] show a strong suppression of different hadron species at high p_t confirming the picture of quenched jets in heavy-ion collisions.

Due to the increased production cross section of high p_t partons at LHC, complementary studies of jet quenching by reconstructed jets become feasible. Originally developed in elementary collisions like e.g. $\mathrm{e}^+ + \mathrm{e}^-$ and p + p collisions [8], reconstructed jets can provide additional information about the angular dependence of jet energy loss due to their sensitivity to both the leading parton and its surrounding parton shower. Results about the medium modification of reconstructed jets at LHC show both a momentum asymmetry between the leading and subleading jet [9, 10] together with strong suppression of reconstructed jets measured by the nuclear modification factor R_{AA} of reconstructed jets [11, 12]. These findings triggered an enormous effort on the theoretical side for describing medium modification of jets [13–18].

Another promising way for studying jet quenching and especially its mass dependence are energetic charm and beauty quarks. Their larger mass and thereby early production time together with their conserved flavor during hadronization makes heavy quarks a clean tool for examining the QGP. However, the actual energy loss mechanism of heavy quarks is actively debated within theoretical models based on pQCD: While in Refs. [19–25] the heavy quarks only scatter elastically and thereby neglect radiative processes, the approaches of Refs. [25–32] also incorporate the possibility of radiative heavy quark processes.

In this letter we combine recent efforts in understanding the medium modification of both heavy quarks [25] and reconstructed jets [16] within the partonic transport approach Bamps (Boltzmann Approach to Multi-Parton Scatterings). To this end, we study the R_{AA} of inclusive and b-tagged reconstructed jets in 0-10% Pb + Pb colli-

*Corresponding author
**Principal corresponding author
Email address: senzel@th.physik.uni-frankfurt.de (F. Senzel)

sions at $\sqrt{s}_{\rm LHC} = 2.76\,\mathrm{A\,TeV}$. B-tagged jets are defined as jets close in angle $\Delta R = \sqrt{\Delta\phi^2 + \Delta y^2}$ to a measured B meson corresponding to beauty quarks and their surrounding shower traversing the medium. As predicted by analytical calculations based on pQCD energy loss [33], first results by the CMS collaboration [34] showed evidence for a suppression of b-tagged jets that is unexpectedly similar to the inclusive jet R_{AA}. These findings could be additionally reproduced in other pQCD energy loss models [35]. To extend these calculations and thereby further discriminate between different heavy quark energy loss mechanisms, we predict the medium modification of jet shapes [36], defined as

$$\rho\,(r) = \frac{1}{\delta r} \left\langle \frac{\sum\limits_{\text{partons} \,\in\, [r_\mathrm{a},\ r_\mathrm{b})} p_\mathrm{T}^{\text{parton i}}}{p_\mathrm{T}^{\text{jet}}} \right\rangle_{\text{jets}} \qquad (2)$$

for reconstructed b-tagged jets in LHC collisions and compare them with results for the inclusive jet shapes by CMS [36]. After normalizing the jet shapes between $r \in [0, R = 0.3]$ to unity, $\rho(r)$ represents the fraction of jet momentum in an angle between $r - \delta r/2$ at r and $r + \delta r/2$ to each jet axis.

The partonic transport approach Bamps describes the QGP created in ultra-relativistic heavy-ion collisions by numerically solving the 3+1 D Boltzmann equation,

$$p^\mu \partial_\mu f(\mathbf{x}, t) = \mathcal{C}_{22} + \mathcal{C}_{2\leftrightarrow 3}\,, \qquad (3)$$

for gluons as well as light and heavy quarks by employing a stochastic test-particle Ansatz [37]. While both the gluons and light quarks (flavor u,d,s) are treated as massless particles, the masses of heavy quarks (flavor c,b) are set to $M_c = 1.3\,\mathrm{GeV}$ and $M_b = 4.6\,\mathrm{GeV}$. By evaluating the running of the QCD coupling on a microscopic level, Bamps considers both elastic and radiative Bremsstrahlung processes: elastic matrix elements that are derived from leading-order pQCD and inelastic matrix elements calculated in an improved Gunion-Bertsch approximation [38] that was recently extended also to massive particles [25]. This procedure allows an equal treatment of massless and massive partons while any potential mass effect results directly from the underlying pQCD matrix element. Thereby, as shown in Ref. [25, 39], the dead cone effect corresponding to a suppression of collinear gluon emissions by a heavy quark is implicitly considered for the full phase space generalizing the seminal work of Ref. [40].

Furthermore, the Landau-Pomeranchuk-Migdal effect [41] corresponding to a suppression of coherent gluon emissions is effectively treated via a theta function $\theta\,(\tau - X_{\rm LPM}\lambda)$ in the inelastic matrix elements, where τ is the formation time of the emitted gluon and λ is the mean free path of the emitting parton. The free parameter $X_{\rm LPM}$ interpolating between the two extreme cases of no LPM suppression ($X_{\rm LPM} = 0$) and the Bethe-Heitler limit of partonic energy loss ($X_{\rm LPM} = 1$) is fixed within this letter to $X_{\rm LPM} = 0.3$ by comparing with the neutral pion R_{AA} data from RHIC [25, 42]. We showed in Ref. [42] that this parameter choice results in a realistic suppression of hadron spectra at both RHIC and LHC while the same interactions also build up a sizable elliptic flow v_2 in the partonic phase. For more details about the Bamps framework and recent results we refer to Refs. [25, 37, 42, 43].

Reconstructed jets are sensitive to the medium modification of both the leading parton and its surrounding shower. Following previous studies about the momentum imbalance A_J of reconstructed jets [16], we employ the event generator Pythia for the initial distribution of parton showers. For the b-tagged jet results we select only events originating from a hard b-quark pair production process while neglecting heavy flavor from gluon splitting processes that are negligible for high p_t bottom production [44]. The parton showers are spatially distributed by a Glauber modeling with a Woods-Saxon density profile and after their formation time subsequently evolved within expanding Bamps simulations of $\sqrt{s}_{\rm LHC} = 2.76\,\mathrm{A\,TeV}$ Pb + Pb collisions with impact parameter $b = 3.6\,\mathrm{fm}$ corresponding to 0-10% centrality.

Based on the medium-modified parton showers, jets are reconstructed by the anti k_t algorithm as provided in the package FastJet [45] while employing different jet radii R. Requiring the same trigger and reconstruction conditions as the experiments, the infra-red safety of the anti k_t algorithm allows a reliable comparison of our parton-level calculations to the measured hadron-level jet data. However, in contrast to the experiments we define a b-tagged jet as a reconstructed jet consisting of a beauty quark instead of only close in angle to a B meson. We checked that these different definitions of a b-tagged jet do not significantly affect the final selection of b-tagged jets at high p_t.

The shower partons—gluons and light quarks—are allowed to scatter both elastically and via Bremsstrahlung processes. However, to further investigate the underlying heavy quark energy loss mechanism we define different scenarios for the b-quark interactions: Consistent with the light partons, in scenario "el.+rad." b-quarks may scatter both elastically and radiatively. In contrast, in scenario "el." the b-quarks may scatter only via elastic processes. This discrimination allows studying the consequences of medium-induced gluon radiation off the b-quark for the reconstructed jets. Furthermore, in order to estimate the mass effect within Bamps we initialize in scenario "$\mathrm{m_{HQ}} = 0$" a b-quark shower within Pythia but consider the beauty quark as massless during the subsequent Bamps evolution. Finally, in scenario "scaled el." we follow our previous studies [25] by employing only elastic heavy quark interactions with a modified Debye screening ($\kappa = 0.2$) together with a scaling factor $K = 3.5$. As discussed in Ref. [25] these scaled elastic interactions describe both the heavy flavor R_{AA} and v_2, while the interactions of scenario "el.+rad." underestimate the flow of heavy quarks.

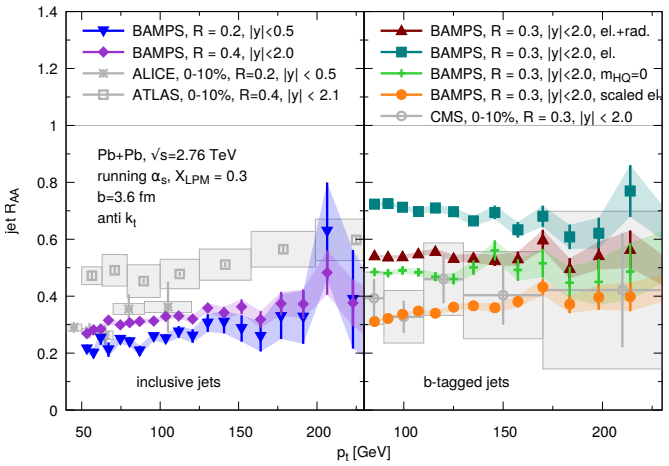
BAMPS, R = 0.2, |y|<0.5
BAMPS, R = 0.4, |y|<2.0
ALICE, 0-10%, R=0.2, |y| < 0.5
ATLAS, 0-10%, R=0.4, |y| < 2.1
BAMPS, R = 0.3, |y|<2.0, el.+rad.
BAMPS, R = 0.3, |y|<2.0, el.
BAMPS, R = 0.3, |y|<2.0, m_HQ=0
BAMPS, R = 0.3, |y|<2.0, scaled el.
CMS, 0-10%, R = 0.3, |y| < 2.0
Pb+Pb, √s=2.76 TeV
running α_s, X_LPM = 0.3
b=3.6 fm
anti k_t
inclusive jets
b-tagged jets
jet R_AA
p_t [GeV]

Figure 1: Nuclear modification factor R_{AA} of inclusive (left) and b-tagged reconstructed jets (right) calculated by BAMPS together with data of 0-10% Pb + Pb collisions at $\sqrt{s}_{\mathrm{LHC}} = 2.76\,\mathrm{A\,TeV}$ [11, 12, 34].

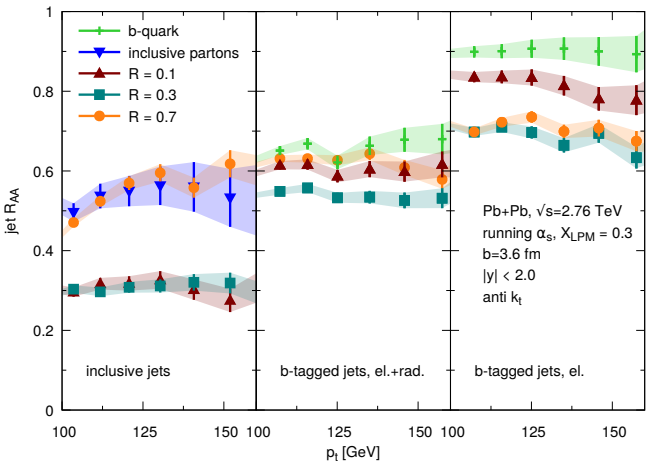

Figure 2: R dependence of the nuclear modification factor R_{AA} of inclusive (left) and b-tagged jets (middle,right) for two different heavy quark energy loss scenarios.

Fig. 1 shows the nuclear modification factor R_{AA} of inclusive (left panel) and b-tagged jets (right panel) calculated within BAMPS together with the corresponding experimental data at LHC. As already found in Refs. [35] the suppression of inclusive and b-tagged jets are on a comparable level. However, the inclusive jet suppression resulting from gluon and light quark jets is too strong in comparison with data for both employed radii $R = 0.2$ and $R = 0.4$. Since BAMPS simulations for the single hadron R_{AA} shows a realistic energy loss of the leading parton [42], this finding shows that the radiated gluons are transported too far away from the respective jet axis within BAMPS.

In the right panel of Fig. 1 we present our results for the b-tagged jet suppression: While only elastic heavy quark processes are insufficient for a realistic jet suppression, the additional medium-induced gluon radiation off the b-quark in scenario "el.+rad." provides an important contribution to the medium transport out of the jet cones. Surprisingly also the scaled elastic heavy quark interactions further enhance the b-tagged jet suppression. Both the increased elastic energy loss and the deflection of the b-quark to larger angles compensates the missing medium-induced gluon radiation off the beauty quark.

Furthermore, by comparing scenario "el.+rad." with scenario "$\mathrm{m_{HQ}} = 0$" and the suppression of inclusive jets one can infer that the different suppression of light and heavy flavor jets is mainly caused by the different initial shower evolution within PYTHIA. The finite mass of the beauty quark during the BAMPS evolution plays at these high momenta only a minor role for the momentum loss of the jets.

To further study the angular dependence of momentum transport out of the jet cones, we show in Fig. 2 the nuclear modification factor R_{AA} of both inclusive (left panel) and b-tagged jets (middle and right panel) for different jet radii $R \in [0.1; 0.3; 0.7]$ in the range $p_t = 100\,\mathrm{GeV} - 170\,\mathrm{GeV}$. The inclusive jet spectra show at first an expectable behavior: A larger radius $R = 0.7$ leads to a decreased jet suppression since gluons transported away from the jet axis are recollected within the jets. Consequently, the lack of these gluons closer to the jet axis leads to a stronger suppression for the smaller radii $R = 0.1$ and $R = 0.3$. Furthermore, the jet R_{AA} within BAMPS is similar for both smaller radii demonstrating again that the medium-modification of inclusive jets is dominated by the large R region. On the contrary, when comparing the jet suppression to the R_{AA} of single inclusive partons (corresponding to the limit $R = 0$), the suppression of spectra decreases again comparable to the jet R_{AA} with $R = 0.7$.

As presented in the middle and right panel of Fig. 2 the R dependence of b-tagged jets shows a slightly different behavior: While the suppression at $R = 0.7$ is moderated again by recollecting gluons at large angles, we predict already for the small radius $R = 0.1$ a weaker jet suppression of b-tagged jets relative to the larger radius $R = 0.3$ for both shown scenarios. This trend is further confirmed by comparing with the bare b-quark suppression (green line). The difference between the smaller radius $R = 0.1$ and the larger radius $R = 0.3$ is even more pronounced in the scenario "el." where medium-induced radiation off the b-quark is neglected.

In order to explain the R dependence of inclusive and b-tagged jet suppression we would like to discuss in the following our picture of jet modification in the QGP, which follows from generic considerations and therefore should also, at least qualitatively, be observable in other energy loss models. In p + p collisions both light and heavy partons from the hard interactions radiate gluons due to their large virtuality. However, since the mass of the beauty quark suppresses gluon emissions at small angles, the initial shower of a beauty quark differs from a light parton shower since its core mainly consists of the leading heavy quark. Therefore when reconstructing jets with a high resolution (small radius) in p + p and subsequently in heavy-

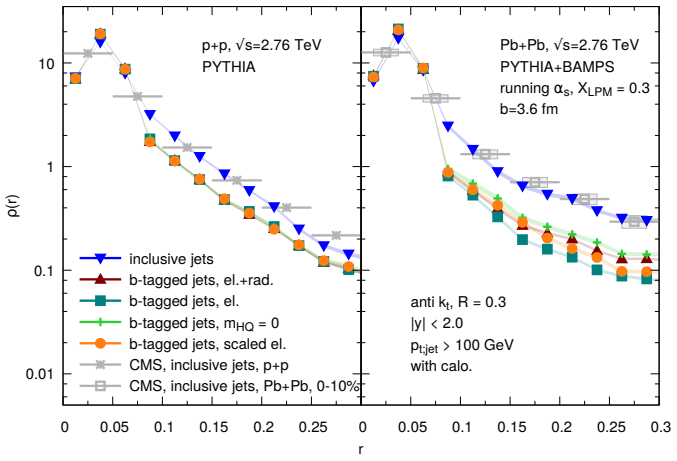

Figure 3: Jet shapes of inclusive and b-tagged jets with $p_{\mathrm{t;jet}} > 100\,\mathrm{GeV}$ calculated by BAMPS with $\delta r = 0.025$ together with data of p + p and 0-10% Pb + Pb collisions both at $\sqrt{s}_{\mathrm{LHC}} = 2.76\,\mathrm{A\,TeV}$.

ion collisions, one measures almost only the modification of the leading beauty quark and not its associated parton shower. In contrast, the core of a jet initiated by a light parton is occupied (light quark initiated) or even dominated (gluon initiated) by shower gluons. Therefore the subsequent transport of these gluons out of the jet cones additionally contributes to the jet momentum loss and thereby to the jet suppression of inclusive jets already at small R. When decreasing the resolution (increasing the radius to e.g. $R = 0.3$) also the b-tagged jets become sensitive to the transport of gluons at intermediate angles out of the jet cones what results in a stronger suppression compared to smaller radii (e.g. $R = 0.1$). This is even more pronounced in scenario "el." where no additional medium-induced gluon radiation off the b-quark is considered. On the contrary, jets initiated by a light parton lack this effect since the gluons of the associated shower are transported to angles larger than $R = 0.3$ resulting in a similar jet suppression from $R = 0.1$ to $R = 0.3$. Only at a small resolution (large radius) the shower gluons of both light and heavy flavor initiated showers are recollected to the jets so that the suppression of both inclusive and b-tagged jets decreases.

In the following, we further develop our picture of jet quenching by studying the medium-modification of jet shapes $\rho(r)$ (cf. eq. 2). In contrast to the results for R_{AA}, jet shapes are more sensitive to the resolution with which the jet axis can be determined since single particles are correlated with the reconstructed jets. Therefore we reconstruct jets from discretized cells in $\Delta\phi$-Δy with bin width 0.1 instead from single partons in order to mimic the finite resolution effects of experimental calorimeters [16, 34]. By comparing with jet shapes based on single partons (not shown) this finite resolution effect leads to "wobbling" jet axes that result in broader jet shape distributions around $r = 0$.

Fig. 3 shows the normalized jet shape distributions from PYTHIA before (left panel) and after evolving within BAMPS (right panel) for inclusive jets and the different b-tagged jet scenarios in comparison with data for p + p and 0-10% central Pb + Pb collisions both at $\sqrt{s}_{\mathrm{LHC}} = 2.76\,\mathrm{A\,TeV}$. Although the calorimeter effects smear the distributions at small r the jet shape distribution of b-tagged jets in p + p collisions is still slightly narrower than the distribution of inclusive jets. This gives additional evidence for b-tagged jets that consist mainly of the leading beauty quark in p + p collisions. After traversing the BAMPS medium both jet shape distributions become flatter at $r > 0.1$ what is consistent with the experimental data for the inclusive jets. However, in contrast to the similar jet R_{AA} of inclusive and b-tagged jets, the jet shape distribution shows a significantly less fraction of jet momentum at $r > 0.1$ for b-tagged than for inclusive jets. This again is caused by the missing gluon radiation of a beauty quark within PYTHIA which results in fewer gluons that can be transported to these angles by the medium. Also the medium-induced radiation of the beauty quark is insufficient for refilling this region as can be seen by comparing the jet shapes of the different b-tagged jet scenarios.

This missing replenishment of gluons at intermediate angles $r > 0.1$ can be further demonstrated in Fig. 4 where we show the ratio of jet shape distributions before and after the BAMPSevolution in comparison with data and thereby predict for the first time the medium-modification of b-tagged jet shapes. On one hand the inclusive jet shapes show an almost unmodified inner jet core that is consistent with data and a too strong enhancement of the distributions at large angles $r > 0.25$ that is consistent with the too strong suppression of inclusive jets within BAMPS. On the other hand, all heavy quark scenarios show around $r \approx 0$ a similar behavior as the inclusive jets and at $r > 0.1$ a depletion resulting from shower gluons transported to larger angles that are not refilled by medium-induced gluon radiation. The different heavy quark interactions lead to a hierarchy of modification at larger $r > 0.25$: The radiative heavy quark processes of scenario A lead to the strongest enhancement of momentum at large r, while elastic processes of scenario B and C are less effective in transporting momentum to these large angles. Furthermore, the similarity of the scenarios "el.+rad." and "$m_{\mathrm{HQ}} = 0$" shows that the jet shapes are dominated by the initial characteristic distribution around the b-quark and not by the finite mass within the BAMPS evolution. With increasing experimental statistics the differences between the elastic and radiative scenarios will be measurable and thereby may provide evidence for the respective underlying energy loss.

In summary, we compared results on the nuclear modification factor of reconstructed inclusive and b-tagged jets in ultra-relativistic heavy-ion collisions obtained from microscopic, non-equilibrium transport calculations. While the suppression of inclusive reconstructed jets seems to be strong in comparison with data from the LHC, the so far measured b-tagged jet R_{AA} does not allow a reliable dis-

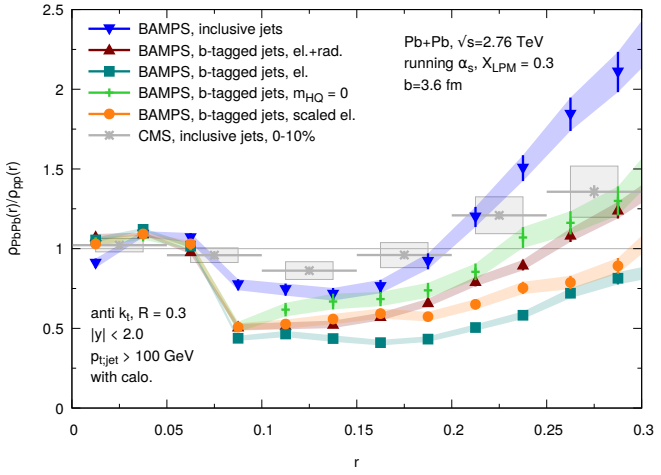

Figure 4: Medium modification of jet shapes of inclusive and b-tagged jets with $p_{\mathrm{t;jet}} > 100\,\mathrm{GeV}$ calculated by BAMPS with $\delta r = 0.025$ together with data of 0-10% Pb + Pb collisions at $\sqrt{s}_{\mathrm{LHC}} = 2.76\,\mathrm{A\,TeV}$.

crimination between scaled elastic and elastic+radiative processes within BAMPS. Furthermore, we predicted the R dependence of the b-tagged jet R_{AA} caused by the suppressed gluon radiation of b-quarks in vacuum and thereby a missing replenishment of gluons at intermediate angles relative to the jet axis. This finding was confirmed by a closer look at the medium modification of inclusive and b-tagged jet shapes. By predicting b-tagged jet shapes we find that their measurement should allow a reliable discrimination between different heavy quark energy loss mechanisms and thereby facilitates a further understanding of the mass dependence of jet quenching.

Acknowledgments: FS thanks R. Bertens for helpful discussions regarding the experimental feasibility. This work was supported by the Bundesministerium für Bildung und Forschung (BMBF), the MOST, the NSFC under Grants No. 2014CB845400, No. 11275103, No. 11335005, HGS-HIRe, and the Helmholtz International Center for FAIR within the framework of the LOEWE program launched by the State of Hesse. Numerical computations have been performed at the Center for Scientific Computing (CSC).

References

[1] J. D. Bjorken, Fermilab PUB-82/59-THY (1982).
[2] P. Braun-Munzinger and J. Stachel, Nature **448**, 302 (2007).
[3] B. V. Jacak and B. Muller, Science **337**, 310 (2012).
[4] PHENIX Collaboration, Phys. Rev. Lett. **88**, 022301 (2002).
[5] STAR Collaboration, Phys. Rev. Lett. **89**, 202301 (2002).
[6] ALICE Collaboration, Phys. Lett. B **696**, 30 (2011).
[7] CMS Collaboration, Eur. Phys. J. C **72**, 1945 (2012).
[8] G. P. Salam, Eur. Phys. J. C **67**, 637 (2010).
[9] ATLAS Collaboration, Phys. Rev. Lett. **105**, 1 (2010).
[10] CMS Collaboration, Phys. Rev. C **84**, 024906 (2011).
[11] ATLAS Collaboration, Phys. Rev. Lett. **114**, 0 (2014).
[12] ALICE Collaboration, Phys. Lett. B **746**, 1 (2015).
[13] J. Casalderrey-Solana, J. G. Milhano, and U. A. Wiedemann, J. Phys. G Nucl. Part. Phys. **38**, 035006 (2011).
[14] K. C. Zapp, F. Krauss, and U. A. Wiedemann, J. High Energy Phys. **1303** (2013) 080.
[15] T. Renk, Phys. Rev. C **85**, 064908 (2012).
[16] F. Senzel, O. Fochler, J. Uphoff, Z. Xu, and C. Greiner, J. Phys. G Nucl. Part. Phys. **42**, 115104 (2015).
[17] L. Apolinário, N. Armesto, and L. Cunqueiro, J. High Energy Phys. **1302** (2013) 022.
[18] M. van Leeuwen, (2015), arXiv:1511.06108 .
[19] P. B. Gossiaux, R. Bierkandt, and J. Aichelin, Phys. Rev. C **79**, 044906 (2009).
[20] J. Uphoff, O. Fochler, Z. Xu, and C. Greiner, Phys. Rev. C **84**, 024908 (2011).
[21] J. Uphoff, O. Fochler, Z. Xu, and C. Greiner, Phys. Lett. B **717**, 430 (2012).
[22] C. Young, B. Schenke, S. Jeon, and C. Gale, Phys. Rev. C **86**, 034905 (2012).
[23] A. Meistrenko, J. Uphoff, C. Greiner, and A. Peshier, Nucl. Phys. A **901**, 51 (2013).
[24] W. M. Alberico, A. Beraudo, A. De Pace, A. Molinari, M. Monteno, M. Nardi, F. Prino, and M. Sitta, Eur. Phys. J. C **73**, 2481 (2013).
[25] J. Uphoff, O. Fochler, Z. Xu, and C. Greiner, J. Phys. G Nucl. Part. Phys. **42**, no. 11, 115106 (2014).
[26] R. Sharma, I. Vitev, and B.-W. Zhang, Phys. Rev. C **80**, 054902 (2009).
[27] R. Abir, U. Jamil, M. G. Mustafa, and D. K. Srivastava, Phys. Lett. B **715**, 183 (2012).
[28] A. Buzzatti and M. Gyulassy, Phys. Rev. Lett. **108**, 022301 (2012).
[29] S. Cao, G.-Y. Qin, and S. A. Bass, Phys. Rev. C **88**, 044907 (2013).
[30] M. Djordjevic and M. Djordjevic, Phys. Lett. B **734**, 286 (2014).
[31] M. Nahrgang, J. Aichelin, P. B. Gossiaux, and K. Werner, Phys. Rev. C **90**, 024907 (2014).
[32] T. Renk, Phys. Rev. C **89**, 054906 (2014).
[33] J. Huang, Z.-B. Kang, and I. Vitev, Phys. Lett. B **726**, 251 (2013).
[34] CMS Collaboration, Phys. Rev. Lett. **113**, 132301 (2013).
[35] M. Djordjevic, B. Blagojevic, and L. Zivkovic, (2016), arXiv:1601.07852 .
[36] CMS Collaboration, Phys. Lett. B **730**, 243 (2013).
[37] Z. Xu and C. Greiner, Phys. Rev. C **71**, 064901 (2005).
[38] O. Fochler, J. Uphoff, Z. Xu, and C. Greiner, Phys. Rev. D **88**, 014018 (2013).
[39] R. Abir, C. Greiner, M. Martinez, M. G. Mustafa, and J. Uphoff, Phys. Rev. D **85**, 054012 (2012).
[40] Y. Dokshitzer and D. Kharzeev, Phys. Lett. B **519**, 199 (2001).
[41] A. B. Migdal, Phys. Rev. **103**, 1811 (1956).
[42] J. Uphoff, F. Senzel, O. Fochler, C. Wesp, Z. Xu, and C. Greiner, Phys. Rev. Lett. **114**, 112301 (2015).
[43] Z. Xu and C. Greiner, Phys. Rev. C **76**, 024911 (2007).
[44] M. Bedjidian *et al.*, arXiv:hep-ph/0311048.
[45] M. Cacciari, G. P. Salam, and G. Soyez, Eur. Phys. J. C **72**, 1896 (2012).